Quaternary International 246 (2011) 298–311

Contents lists available at SciVerse ScienceDirect

Quaternary International

journal homepage: www.elsevier.com/locate/quaint

Tephrochronological investigation at Dvuh-yurtochnoe lake area, Kamchatka: Numerous landslides and lake tsunami, and their environmental impacts

O. Dirksen[a,*], C. van den Bogaard[b], T. Danhara[c], B. Diekmann[d]

[a] Institute of Volcanology and Seismology FED RAS, Piipa blvd., 9 Petropavlovsk-Kamchatsky 683006, Russia
[b] Leibniz-Institut für Meereswissenschaften, IFM-GEOMAR, Wischhofstr 1-3, 24148 Kiel, Germany
[c] Kyoto Fission Track Co. Ltd., 44-4 Minamitajiri-cho, Kita-ku, Kyoto 603, Japan
[d] Alfred-Wegener-Institute für Polar-und Meeresforschung (AWI), Telegrafenberg A43, 14473 Potsdam, Germany

ARTICLE INFO

Article history:
Available online 27 August 2011

ABSTRACT

Distal volcanic tephras in soil sections and lake sediments in the Dvuh-yurtochnoe (Two-Yurts) lake area, central Kamchatka, were investigated in order to provide a chronological framework for the reconstruction of late Quaternary landscape development. Mineralogical and geochemical data point to sources from 5 volcanoes. Ten tephra layers were identified and correlated to known eruptive events. The ages were corroborated by radiocarbon dating of the soil sections around Two-Yurts lake. These findings allow the reconstruction of regional paleoenvironmental change, recorded in the soil sections around Two-Yurts lake. During the Last Glacial Maximum (LGM) time, the area was affected by glacial advances that produced the glacial moraines at the eastern outlet of the lake. A large landslide, ca. 15,000–18,000 ^{14}C BP, dammed the valley and led to formation of Two-Yurts lake. Several more landslide events can be recognized in the Holocene, and one affected Two-Yurts lake ca. 3000 ^{14}C BP. This event produced a "tsunami", documented by poorly sorted deposits with rounded pebbles in the onshore sections around the lake. In contrast to the soil sections, tephras buried in the "soupy" lacustrine sediments of Two-Yurts lake are not well preserved and show inconsistent age-depth relationships compared to those suggested by radiocarbon dating, due to sinking through the lake sediments. Nevertheless, tephrochronological data revealed the strong impact of terrestrial landslides on lake sedimentation.

1. Introduction

A regional tephrochronological framework began to develop in Kamchatka in the 1980s (Braitseva et al., 1980). The first summary of Kamchatka marker tephra layers (Braitseva et al., 1997) reported 24 main tephras, found mainly in southern and eastern Kamchatka. Recent publications significantly enlarged the number of well-dated marker tephra layers in Kamchatka (Braitseva et al., 1998; Dirksen et al., 2002; Bazanova et al., 2004, 2005). Investigations on tephra stratigraphy in different areas of Kamchatka allowed researchers to construct detailed tephrochronological schemes for different parts of Kamchatka and use them for reconstruction of the eruptive history of Kamchatka stratovolcanoes (Melekestsev et al., 1995; Bazanova and Pevzner, 2001; Bazanova et al., 2003; Ponomareva et al., 2007b) as well as dating different natural events such as tsunami, landslides, and eruptions of monogenetic cinder cones (Melekestsev and Kurbatov, 1998; Dirksen and Melekestsev, 1999; Pinegina et al., 2003; Bourgeois et al., 2006). Some attempts were also made to use tephrochronology for dating paleoclimatic events (Savoskul and Zech, 1997). However, most investigations were carried out in central and eastern Kamchatka. Application of this method in the Dvuh-yurtochnoe (Two-Yurts) lake area, the focus of paleoenvironmental studies under the umbrella of the Russian-German KALMAR project ("Kurile Kamchatka and Aleutean Marginal Sea – Island Arc Systems: Geodynamic and Climate Interaction in Space and Time"), required the collection of new data as well as improving modern knowledge on the distribution of some marker tephra layers in central Kamchatka. Application of tephra stratigraphy could provide a suitable tool to ensure age determination of palaeoenvironmental archives, such as soil and peat sections as well as lake deposits.

2. Regional setting

Dvuh-yurtochnoe (Two-Yurts, TYL) lake is a freshwater lake in the north-central part of the Kamchatka peninsula (56 °48′40″N,

* Corresponding author.
E-mail addresses: dirksen@kscnet.ru (O. Dirksen), cbogaard@ifm-geomar.de (C. van den Bogaard), kyoto-ft@ac.auone-net.jp (T. Danhara), Bernhard.Diekmann@awi.de (B. Diekmann).

1040-6182/$ – see front matter © 2011 Elsevier Ltd and INQUA. All rights reserved.
doi:10.1016/j.quaint.2011.08.032

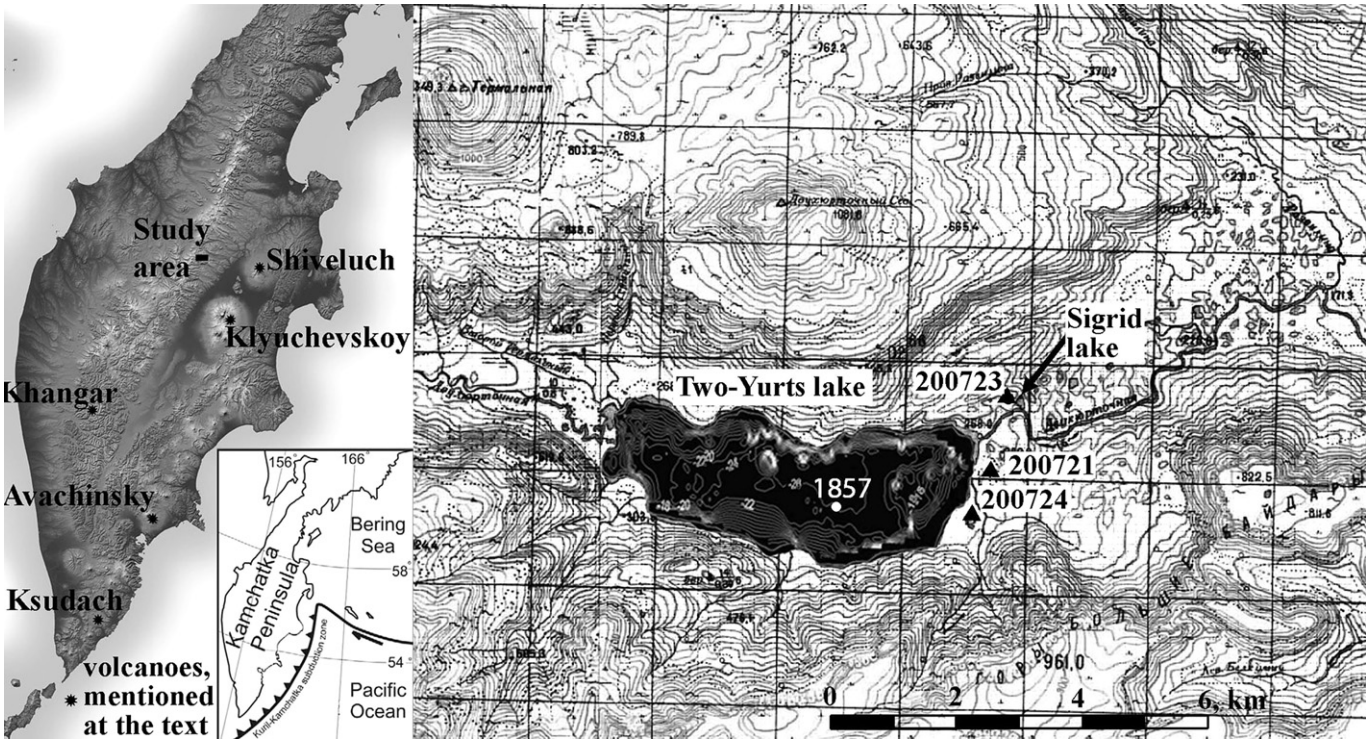

Fig. 1. TYL area with bathymetric map of the lake. Isobaths are shown with 2 m intervals. Positions of studied sites are indicated. Source-volcanoes for the tephras in the TYL area are shown on the regional map.

160°03′20″E, 270 m a.s.l.) (Fig. 1). It occupies part of the inter-mountain depression at the eastern slope of Sredinny Ridge, the most pronounced watershed in Kamchatka, stretching more than 700 km along the peninsula axis. The lake has an area of 12 km^2 and a maximum depth of c. 25 m. It is the source of the Dvuh-Yurtochnaya River which travels 75 km and flows into the Kamchatka River, the biggest river on the peninsula.

Voluminous volcanic activity at this area during the Late Pliocene – Early Pleistocene (Ogorodov, 1972) deposited strata, with Late Pliocene-Early Quaternary pyroclastic deposits armored with a thick package of Early Pleistocene lava flows, building a sub-horizontal plateau-like surface (Fig. 2). This surface was later disrupted by intense faulting in the Middle – Late Pleistocene (Ogorodov, 1972). During the Late Pleistocene, Sredinny Ridge was one of the main sources for glaciation in Kamchatka (Bigg et al., 2008). The glaciers eroded most of the inter-mountain depressions and created valleys oriented NW-SE. Thick LGM glaciers spread along Two-Yurts valley and deposited two end moraines 20 km downstream of the lake (Ogorodov, 1972).

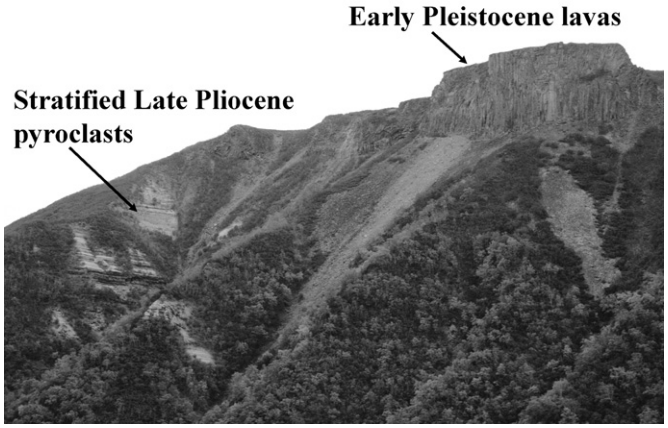

Fig. 2. Geological structure of Two-Yurts area: sequence of Early Pleistocene lavas covers a thick package of loose stratified Late Pliocene-Early Quaternary pyroclasts.

3. Material and methods

During field work, geomorphological features seen on topographic maps and aerial photographs were checked by visual inspection in the field. Six pit sections were dug at representative sites on ancient lake terraces, moraines, and suspected landslide deposits along the eastern end of TYL. In addition, tephra layers from 3 sediment cores of TYL and a nearby small lake were investigated.

The mineralogical study of tephras was carried out at Kyoto Fission Track Co. Part of each tephra sample, about 30 g, was washed on a 63 μm sieve. Further quantitative analysis was conducted of tephra particles between the 63- and 125-μm meshes. Concentration of volcanic glass shards was determined under a binocular microscope. Bulk total mineral and heavy mineral compositions were determined from up to two hundreds grains for every assemblage under the polarizing microscope. Analyses of mineralogical data included the following minerals: olivine (Ol), orthopyroxene (OPx), clinopyroxene (CPx), brown and green hornblende (BHb and GHb, respectively), opaque minerals (Opq), cummingtonite (Cum), zircon (Zr), biotite (Bt), and apatite (Ap). In some cases, the overall composition of the tephras was considered, which included the percentage of fresh volcanic glass (VG), light mineral fraction (LM), heavy mineral fraction (HM), lithics (non-vesiculated glass shards) and non-identified clasts (Oth). In some cases the results of mineralogical analyses of tephras from lake cores imply probable secondary contamination during deposition through lake sediment or redeposition of older tephras. However,

in most cases the mineral assemblage of the tephras can be used for tephra identification.

Geochemical analyses of the volcanic glass for the terrestrial tephras were conducted at Fukushima University, Japan. The major element compositions of glasses were analyzed with a JEOL JSM-5800LV attached JEOL superminicup semiconductor detector and Oxford Link ISIS EDX at the University of Fukushima. Operating conditions are as follows: an accelerating voltage of 15 kV and a beam current of 0.3 nA with a focused 5 μm diameter beam. Standardization was achieved using the glass standards analyzed by XRF (Nagahtephrai et al., 2003). All the results were normalized to 100% on a water-free basis.

The chemical composition of glass shards from lake core tephras was analyzed with a JEOL electron microprobe at IFM-GEOMAR, Kiel. Analytical conditions were 15 kV accelerating voltage, 6 nA beam current and 20 s of peak counting time (Na, Si, P, Fe, Mg, Al, Ca), 30 s (S, K Cl Ti) Mn (40 s), 10 s on background. Analyses were performed with a ~5 μm electron beam. Participation in the laboratory intercomparison study showed the analytical conditions to be among the top 5 labs (Kuehn et al., in press). For interpretation, only analyses with totals better than 95% were accepted. Data show representative analyses normalized to 100% on a volatile-free basis. Full details on lab conditions and data sets are available on request. In spite of differences in procedure between two laboratories, the results of analyses correspond rather well, as well as to published results on glass chemistry of Kamchatka tephras.

Radiocarbon (^{14}C) AMS (Accelerator Mass Spectrometry) dating was done on 5 samples of buried charcoals from terrestrial sections and 16 samples of lake gyttia from lacustrine cores at the Poznan Radiocarbon Laboratory, Poland (Table 1). Radiocarbon measurements were subsequently converted into calendar ages BC/AD (0 cal. BP = AD 1950), using the CalPal Online program (Danzeglocke et al., 2010).

4. Results and discussion

4.1. Sections

The relief of the study area was formed by the combined effect of two main processes: intense volcanic and tectonic activity during the Early to Late Pleistocene, and extensive Late Pleistocene glaciations. The landscape consists of a wide lava plateau with remnants of volcanic edifices dissected by steep valleys 500–600 m deep. Detail inspection of large-scale air-photo images, analyses of topography, and geological maps revealed several landslides of two types: 1) depression fills with typical hummocky relief, and 2) intact blocks representing downhill sliding of pieces of lava plateau, which retained their initial structure. To date these events, three soil-pyroclastic sections were studied in detail. Two were situated on the surface of the landslide deposits, and the third on the 3 m high lake terrace, at the eastern shore of the lake. The sections range in thickness from 0.8 to 2 m, and represent an intercalation of volcanic tephras with slightly humified brown sandy loams. Charcoals, dispersed within the sandy loams or concentrated to form some lenses, were collected for radiocarbon dating.

Table 1
Radiocarbon dates and calibrated calendar ages of analyzed samples from terrestrial soil-pyroclastic sections and lake cores, Two-Yurts lake area.

Lab Code	Core/Section Code	Core/Section Depth (cm)	Radiocarbon Date (^{14}C BP)	Calibrated Age (cal. BP)
Poz-24129	200,721/A1	30	2040 ± 35	2006 ± 50
Poz-24131	200,723/A1	64	2865 ± 35	2995 ± 55
Poz-24132	200,723/A2	118	4890 ± 40	5632 ± 26
Poz-24133	200,723/A3	169	8320 ± 50	9346 ± 68
Poz-24134	200,723/A4	173	8360 ± 50	9384 ± 63
Poz-31549	1857–2	6	110 ± 30	142 ± 97
Poz-36399	1857–2	78	1375 ± 35	1304 ± 17
Poz-29020	1857–2	119–122	2435 ± 30	2526 ± 130
Poz-36401	1857–2	175	2460 ± 35	2551 ± 117
Poz-29021	1857–2	219–221.5	2960 ± 35	3141 ± 59
Poz-27003	1857–2	252	8060 ± 50	8925 ± 50
Poz-27002	1857–5	12	2010 ± 35	1963 ± 38
Poz-36400	1857–5	70	2475 ± 35	2574 ± 100
Poz-29022	1857–5	129–131.5	3250 ± 35	3484 ± 54
Poz-31550	1857–5	161–162	3660 ± 35	3999 ± 64
Poz-31551	1857–5	202–203	3980 ± 40	4465 ± 43
Poz-24212	1857–5	221	6570 ± 50	7489 ± 43

4.2. Lake sediments

Cores of TYL sediment were obtained from a floating platform in different parts of the lake. Two cores (1857–2 – upper core and 1857–5 – lower core) consist of diatom-rich oozes of rather soupy consistency. They were taken from site 1857, situated in the central part of the lake with depth about 25 m (Fig. 1) within the area of gentle hummocky bottom topography. The detailed sedimentological characteristics of the cores are described in Hoff (2010). A third core was obtained from a small lake (56 °49′38″N, 160°06′52"E, 270 m a.s.l.) which fills a small depression within a hummocky surface of the largest landslide deposit in the Two-Yurts river valley (Fig. 1). The lake has no official name. During field work, it was informally named 'lake Sigrid', a name also adopted in this paper. The almost triangular-shaped lake Sigrid is 250–150 m in size with a maximum depth of about 5 m. The core is 1 m long and consists of gyttja with several intercalated tephra layers. The lowermost, 3 cm thick, interval of the core section consists of basal clay.

4.3. Section tephrostratigraphy

The nearest eruptive center to TYL is Shiveluch volcano, one of the most active Kamchatka volcanoes. More than twenty tephras were distributed to the west of Shiveluch and probably reached the area of investigation. Several marker tephras were also found in northern Kamchatka, originating from other source-volcanoes (Braitseva et al., 1989, 1997): tephra of Opala volcano (1500 ^{14}C BP), two tephras of Ksudach volcano (KS_1 and KS_2, formed 1800 and 6000 ^{14}C BP, respectively), Khangar volcano tephra (6900 ^{14}C BP), as well as two tephras of Avachinsky volcano with ages of ca 3500 and 5500 ^{14}C BP, respectively. All these tephras have distinct petrological features which allowed correlation to the source volcano. However, identification of tephras from the same sources is difficult, due to their similar chemical and mineralogical characteristics. Volcanic tephras from Shiveluch are the most difficult case, and cannot be distinguished by their major element composition (Ponomareva et al., 2007b; Kyle et al., 2011).

In the area around TYL, there are more than 30 tephra layers in the sections (Fig. 3). Most of these tephras are fine grained, and a few have significant admixtures of medium grained grains. Most are pale yellow, although some are dark gray and one is dark orange. The thickness of the layers ranged from millimeters to 7 cm. The tephras were correlated based on their field characteristics (thickness, coarseness, color, and stratigraphic position) as well as their geochemical and mineralogical composition.

Analyses of mineralogical and geochemical data revealed two groups of tephras (Fig. 4). Tephras of the first group (# 21/1, 21/2, 21/4, 23/1, 23/2, 23/3, 23/4, 23/6, 23/7) have similar heavy mineral compositions. The tephras are characterized by a significant predominance of green hornblende (50–80%), large amounts of opaque minerals (10–26%), prevalence of orthopyroxene (8–16%)

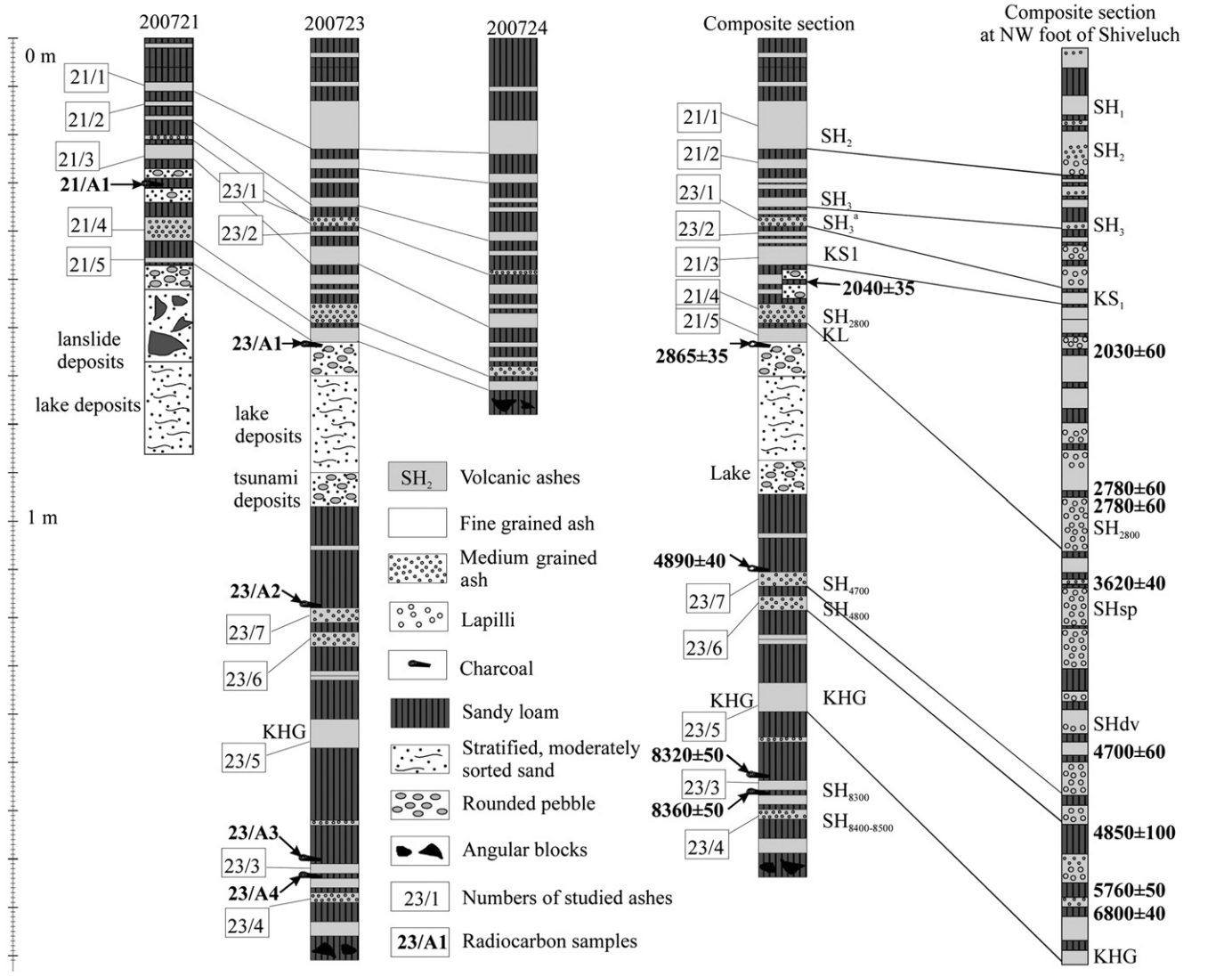

Fig. 3. On-shore soil-pyroclastic sequences and composite section for TYL area. Identified tephras and radiocarbon dates are indicated. Simplified composite section at NW foot of Shiveluch volcano after Ponomareva et al. (2007).

over clinopyroxene (0–4.5%), with trace amounts of olivine and brown hornblende. Tephra #21/2 contains some grains of apatite and tephra #23/3 contains some grains of biotite. Groundmass glasses of these tephras correspond to medium-K rhyolites (3.0–3.5 wt.% K_2O), with SiO_2 content ranging from 73 to 77 wt%. These features correspond to the published data of the tephras of Shiveluch volcano (Braitseva et al., 1997; Ponomareva et al., 2007b; Kyle et al., 2011) (Fig. 5). Therefore, tephras of this group are correlated to the Shiveluch volcano. Nine different Shiveluch tephras were identified and used for correlation between the sections. Age determination is based on correlation of the tephras with dated ones in reference profiles at the foot of the Shiveluch volcano (Ponomareva et al., 2007) and radiocarbon dating of charcoals found in the sections.

In the upper parts of the sections, four tephra layers are noticeably different from other ones. Layer # 21/1, a fine grained tephra, has the maximum thickness of all the tephras in sections around the lake; in some cases it reaches 10 cm. Available data on isopach maps of some Late Holocene Shiveluch tephras (Ponomareva et al., 2007; Kyle et al., 2011) suggested that two tephras of this volcano should be found in the TYL area: SH_1 and SH_2, formed ca 250 and 950 ^{14}C BP, respectively. However, detailed inspection of published data on the proximal sections at SSW and NW sectors of the volcano (Ponomareva et al., 2007, Fig. 7), where SH_2 is much thicker than SH_1, allowed correlation of layer # 21/1 to SH_2 tephra formed ca 950 ^{14}C BP (Braitseva et al., 1997).

Below the SH_2 tephra is another prominent tephra layer. It is 2-cm thick in most of the sections around the lake, and shows distinct normal grading. Following the description of Ponomareva et al. (2007), this tephra is correlated to SH_3 (ca 1400 ^{14}C BP) which shows similar grading in most known sections except in the most distal ones (Braitseva et al., 1997; Ponomareva et al., 2007).

The third tephra layer (#23/1) is a relatively thick (1–2 cm) and medium grained tephra which has a “salt-and-pepper” appearance, typical for the tephras of Shiveluch (Bourgeois et al., 2006). This tephra is correlated with tephra #18 in the sections at the NW sector of Shiveluch (see Ponomareva et al., 2007, Fig. 7). The age of this tephra ranges from 1700 to 1800 ^{14}C BP, probably around 1750 ^{14}C BP as was established for SH_a^3 tephra (Ponomareva et al., 1997).

The last tephra (# 21/4) at the upper part of the section is a medium grained 2–4 cm thick tephra, and is correlated to tephra

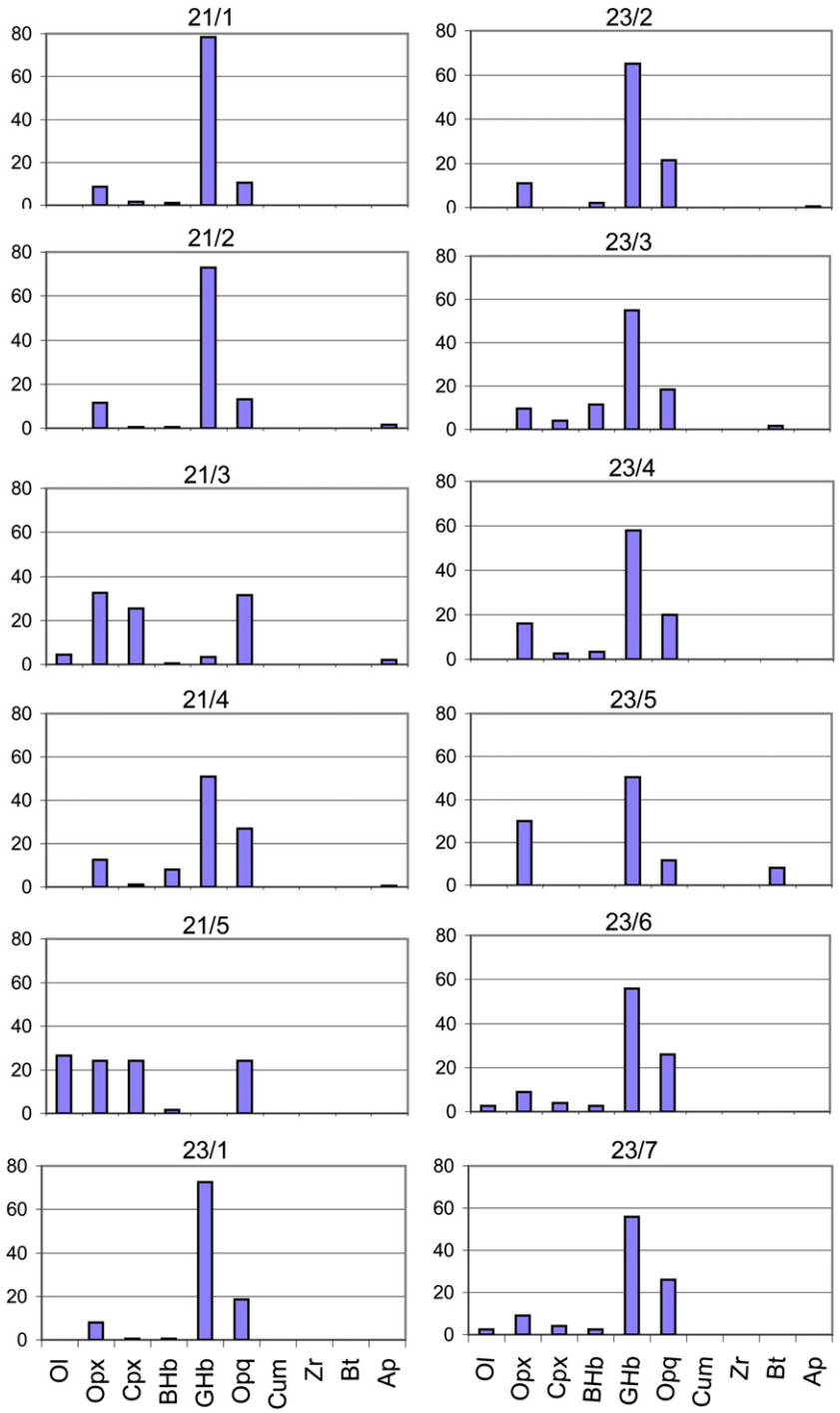

Fig. 4. Mineralogical histograms for the terrestrial tephras. Abbreviation for the minerals: Ol – olivine, OPx – orthopyroxene, CPx – clinopyroxene, BHb – brown hornblende, GHb – green hornblende, Opq – opaque minerals, Cum – cummingtonite, Zr – zircon, Bt – biotite, Ap – appatite. Samples are indicated using the tephra numbers (Fig. 3).

SH_{2800}, described from the foot of Shiveluch (Ponomareva et al., 2007, Fig. 7). The radiocarbon date of 2865 ± 35 ^{14}C BP below this tephra supports this identification.

Two medium grained tephras layers (#23/7 and 23/6) at the middle part of the composite section were correlated using a composite section for Shiveluch volcano (see Ponomareva et al., 2007, Fig. 9). These older tephras are radiocarbon dated to 4890 ± 40 BP, obtained from the charcoal-rich lens just above the tephras. These are correlated to the Shiveluch tephras, which have ages of 4700 and 4800 ^{14}C BP, respectively.

Three tephras from the lower part of the sections (# 23/3 and two tephras below) cannot be correlated with any known tephras of Shiveluch with confidence. Strong explosive activity of Shiveluch Volcano in the early Holocene between 7000 and 10,000 ^{14}C BP resulted in the deposition of 17 tephras in the proximal area around the volcano. However, the stratigraphy of these tephra layers has not been studied. Two radiocarbon dates obtained from the sections around TYL suggest that the tephra # 23/3 formed at about 8300 ^{14}C BP, and the two lowermost tephras were deposited around 8400–8500 ^{14}C BP.

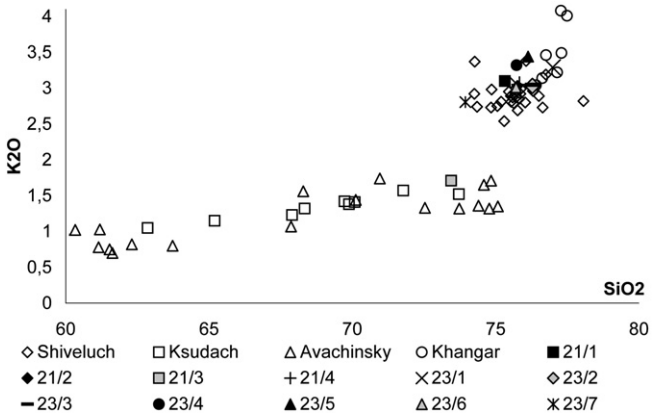

Fig. 5. Potassium (K_2O) versus silica (SiO_2) content (in wt%) of electron microprobe analyses of glass in the tephras from sections. The numbers correspond to the tephra numbers in Fig. 3. Data for glass composition of Shiveluch, Avachinsky, Ksudach and Khangar tephras were taken from Volynets et al. (1999), Ponomareva et al. (2007), and Kyle et al. (2011).

(2) The second group of volcanic tephra layers encountered in sections around TYL comprises three tephras with differing mineralogical composition.

Tephra # 21/3 represents a pumiceous fine grained tephra layer with a yellow lower part and greyish upper one. It has large amount of pyroxene (58%) with a prevalence of orthopyroxene over clinopyroxene. Opaque minerals comprise 31.5%. The tephra also contains olivine (4.5%), green hornblende (3.5%) and apatite (2%). Groundmass glasses of the tephra correspond to low-K rhyolites with SiO_2 content of 73.45 ± 0.34 wt/% (Fig. 5). These features fit well with the characteristics of a marker tephra of Ksudach volcano, formed 1800 ^{14}C BP (KS_1), except for the presence of GHb and Ol. Finding hornblende in KS_1 tephra is rather unusual. Most published results reported the absence of hornblende as a main charateristic feature of KS_1 tephra (Braitseva et al., 1996, 1997; Volynets et al., 1999). This may indicate some contamination of KS1 tephra with crystals (Hb and Ol) from other source. There is limited data on the presence of juvenile Hb in KS_1 tephra (Dirksen et al., 2006), also in small amounts. The presence of Ol could be the result of contamination. Thus, the origin of Hb and Ol crystals in KS1 tephra (juvenile or redeposited) is debatable and requires additional investigation.

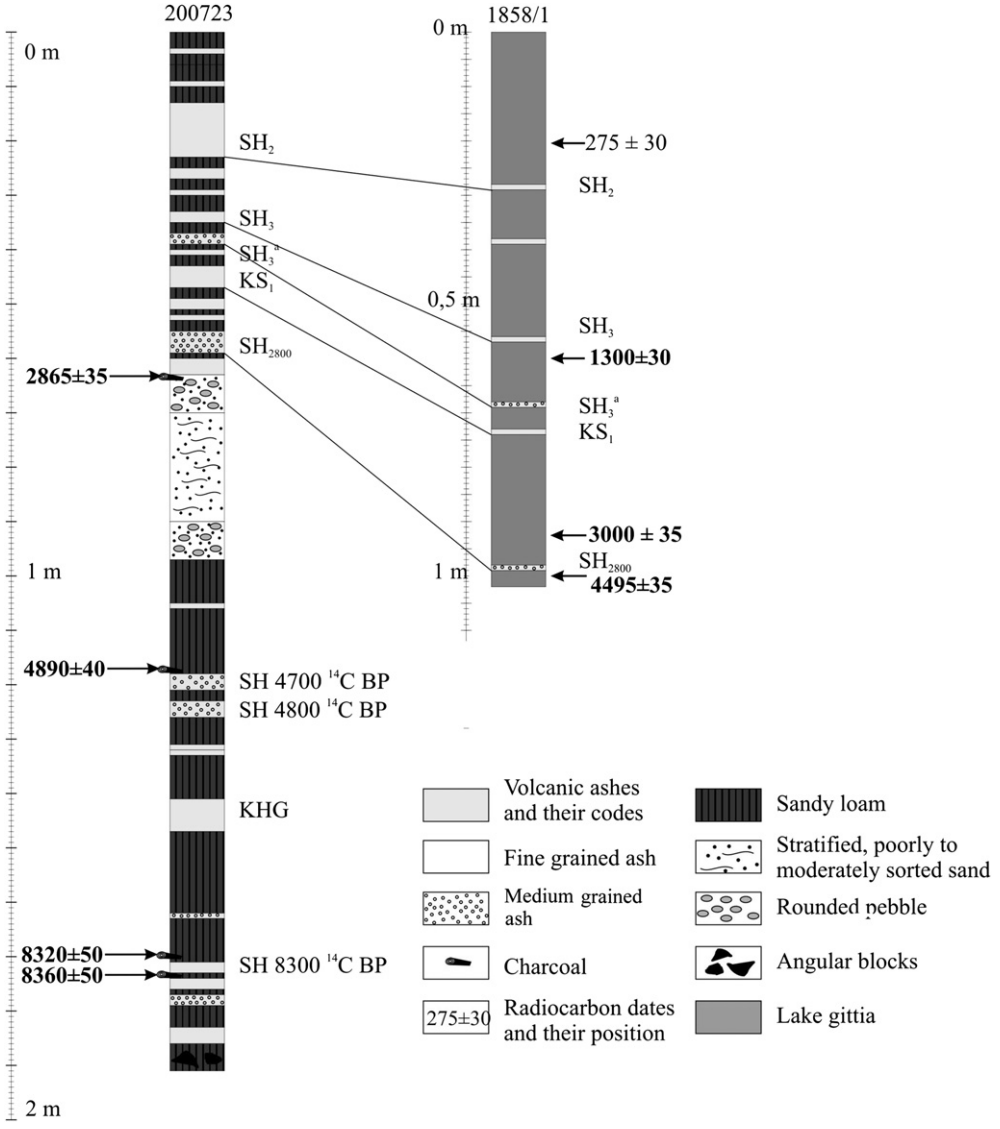

Fig. 6. Correlation of tephras of 1858/1 lake sediment core with tephra layers of section 200723.

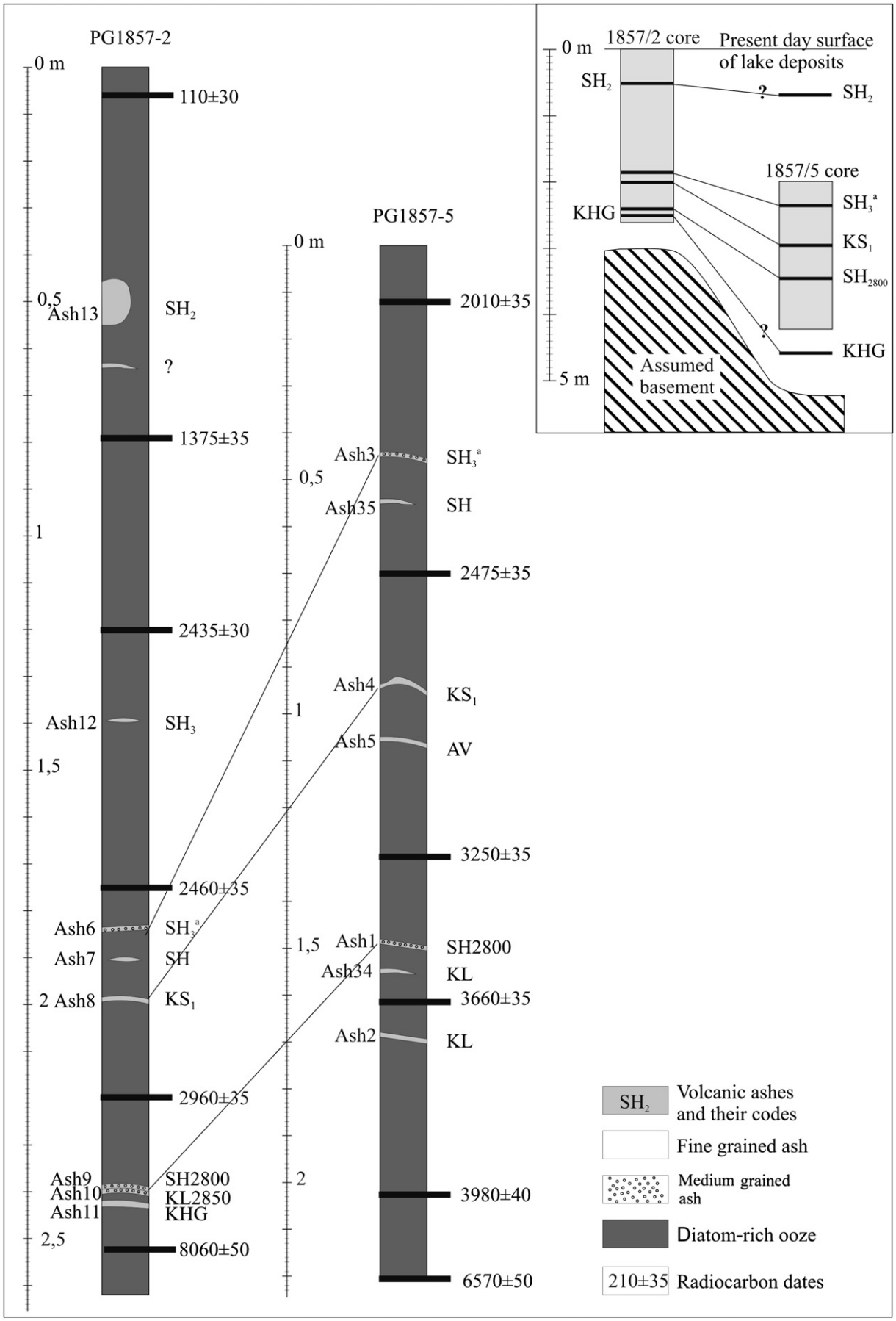

Fig. 7. Correlation of lacustrine cores 1857/2 and 1857/5 and their possible relative position.

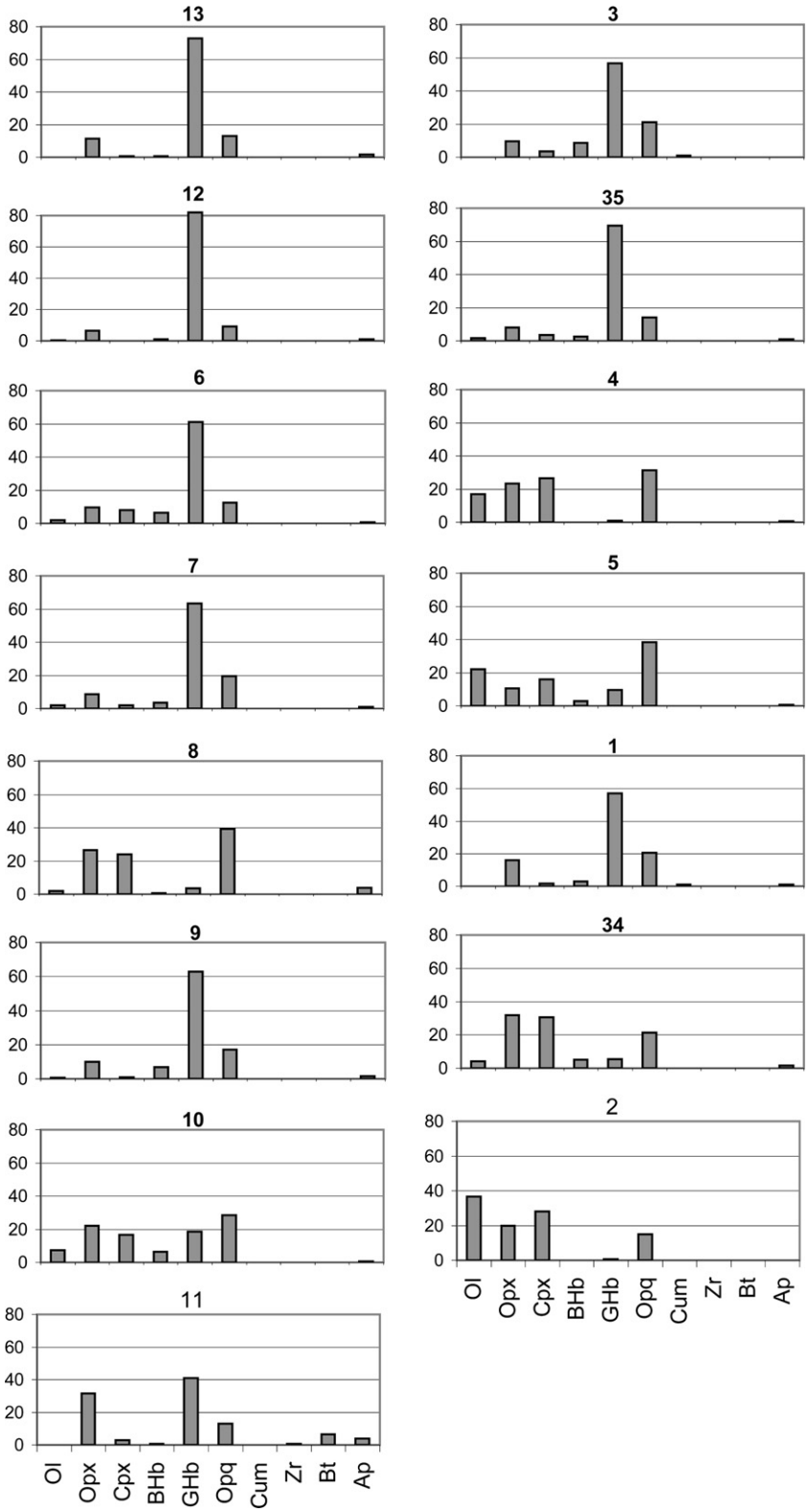

Fig. 8. Mineralogical histograms (percentage to total amount) for tephras in cores 1857/2 and 1857/3. Tephra labels correspond to the tephra numbers in Fig. 7. Abbreviations for the minerals: see Fig. 4.

Attribution of the tephra # 21/3 to Avachinsky volcano, which also produces low-K silicic tephras, can be ruled out, because the tephras of this volcano usually contain larger amounts of GHb. Volcanic glass of the tephra erupted in this time interval is more basic in composition and has higher amounts of K_2O (Braitseva et al., 1989, 1997; Bazanova et al., 2005). The position of this tephra in the upper part of the sections as well as the radiocarbon date below (2040 ± 35 ^{14}C BP) also supports correlation with Ksudach KS_1 tephra.

Tephra # 21/5 (KL) is a fine grained, dark gray tephra (0.2–1 cm thick) that contains a distinct set of heavy minerals. Olivine is most

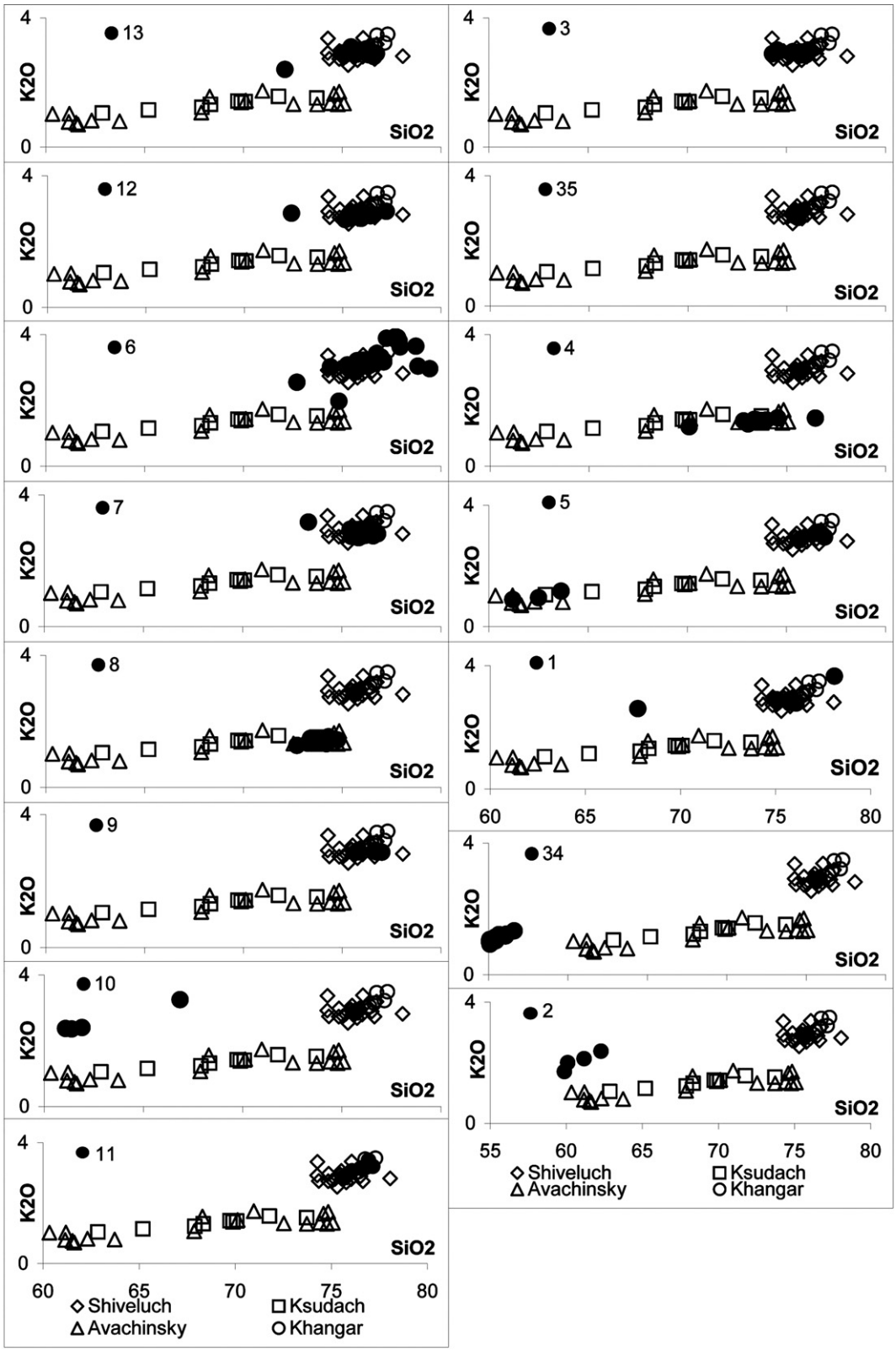

Fig. 9. Potassium (K_2O) versus silica (SiO_2) content (in wt%) diagrams of electron microprobe analyses of glass for tephras in lake sediments. Tephra labels correspond to the tephra numbers at Fig. 7. Data for glass composition of Shiveluch, Avachinsky, Ksudach and Khangar tephras were taken from Volynets et al. (1999), Ponomareva et al. (2007), and Kyle et al. (2011). Note the different scale of SiO_2 axis for the last two diagrams.

abundant (26.5%). Ortho- and clinopyroxene contents are high (both 24%), as well as opaque minerals (24%). Brown hornblende amounts to a few grains (1.5%). The tephra also contains a large amount of non-vesiculated glass shards (94% of overall composition). This was not observed in any distal marker tephra, but published data on the basalts of Klyuchevskoy volcano reported similar mineral assemblages (Ozerov et al., 1996). Therefore, tephra # 21/5 is considered to originate from the eruptions of Klyuchevskoy volcano. This volcano is situated 90 km from the lake, and some distal tephras could reach this area. A radiocarbon date obtained from the charcoal, found directly below the tephra, yielded the age of 2865 ± 35 ^{14}C BP, suggesting that the eruption occurred about 2850 ^{14}C BP. Unfortunately, no fresh volcanic glass shards were found in the sample, which did not allow confirmation of this identification by geochemical data.

Tephra # 23/5 is a fine grained dark orange tephra, 2–6 cm thick, found in the lower part of the sections. Two radiocarbon dates obtained determine that the age of this tephra lies between 4890 ± 40 and 8320 ± 50 ^{14}C BP. Its mineral assemblage is characteristic: besides the large percentages of green hornblende (50%) and orthopyroxene (30%), it contains a large amount of biotite (8%). Groundmass glasses of the tephra correspond to medium to high-K rhyolites (SiO_2 ranges from 75 to 77 wt%). Although the geochemical composition of this tephra is rather close to those of Shiveluch volcano (Fig. 5), the large amount of biotite crystals indicates an origin from another volcano. Two biotite-rich distal tephras were reported by Braitseva et al. (1997): OP – tephra of Barany Amphitheater (Opala volcano), 1500 ^{14}C BP, and KHG tephra of Khangar volcano, 6900 ^{14}C BP. Considering all these data, this tephra is correlated to the KHG tephra, 6900 ^{14}C BP.

4.4. Tephrostratigraphy of lake sediments

In sediment core PG 1858–1 from lake Sigrid, four tephra layers have been identified. They form distinct sub-horizontal layers with sharp boundaries and range in thickness between a few millimeters and 5 cm. Four radiocarbon dates were obtained to build the depth-age model for the core. Four tephras were recognized at this core and correlated with the nearest terrestrial section, 200,723: SH_2, SH_3, KS_1 and SH_{2800} (Fig. 6). This determines the age of the lake as ca. 3000 ^{14}C BP in spite of the older dates at the bottom of the core (see below). The tephra stratigraphy fits very well with radiocarbon dates obtained at the core, except for the two oldest dates. However the amount of visually detected tephra horizons in the lake sediment core is smaller compared to the onshore 200,723 site, which is just 20 m away (6 and 13, respectively, for the last 3000 ^{14}C years).

Nine tephra layers were discovered in core PG1857-2, and seven tephra layers in core PG1857-5. These records can be spliced together and correlated according to the characteristics of the tephra layers (Fig. 7). The tephras identified in the cores are mostly fine – to medium grained. Most are pale yellow, although some are gray. The thickness of single layers ranges from few millimeters to 7 cm. Many tephras form discontinuous lenses and patches.

The SH_2, SH_3, SH_3^a, KS_1, SH_{2800}, KL (2850 ^{14}C BP) and KHG tephras were recognized (Figs. 8 and 9). The close spacing of three tephras: SH_{2800}, KL (2850 ^{14}C BP) and KHG is rather unusual. Although identification of the KHG tephra is robust due to its mineralogical characteristics and glass chemistry, the attribution of two other tephras (#9 and #10) requires additional explanation. The upper medium grained tephra (#9) contains mainly medium-K rhyolite glass and heavy mineral composition characteristic of the Shiveluch tephras. The lower tephra (#10) contains few volcanic glass shards (<1%), a large amount of lithics (>75%) and a specific set of heavy minerals: Opq (28%), OPx (22%), GHb (18%), CPx (16.5%), Ol (7.5%) and BHb (6.5%). This composition is characteristic for Klyuchevskoy volcano tephras (Ozerov et al., 1996; Krasheninnikov et al., 2009; Portnyagin et al., 2009). The onshore sections show two closely spaced tephras (SH_{2800} and KL) with similar features which allowed correlation of tephra #9 to SH_{2800} and #10 to KL. Based on geochemical and mineralogical results, tephra # 5 probably originated from Avachinsky volcano, and tephras # 34 and 2 from Klyuchevskoy volcano, but the ages of these tephras are not clear.

Similar to the lake Sigrid record, the amount of tephra layers in the sediments of TYL is smaller than the number of tephras in the onshore sections. In core PG1857-2, for instance, eight tephras were deposited in the last 3000 ^{14}C years, whereas sixteen tephras are present in onshore sections for the same time interval. Characteristically, the tephras in the subaerial environments form distinctive sub-horizontal layers, whereas they are contorted and slurried in the lacustrine sediments, especially in TYL. It seems that TYL had less favorable conditions for tephra preservation in comparison to on-land sections. Some additional disturbance could arise from syn-earthquake deformation of the lake deposits (Wetzler et al., 2010).

Two points call the tephra identification into question: 1) significant inconsistency between the age of the tephras and radiocarbon dating, and 2) the presence of the younger tephras in the lower core, compared to the lowermost tephra found in the upper core. From the depth-age curve for the upper part of core PG1857-2 (Fig. 10), most of the tephras (except for SH_2) are significantly deeper than contemporaneous lacustrine deposits. It is very important for tephrochronological investigation as well as for paleoenvironmental reconstruction to figure out the possible reasons for this discrepancy. The possibility of constant error in radiocarbon dating is excluded, as results yielded very appropriate dates for terrestrial deposits as well as for the lake deposits of Sigrid lake.

Two plausible reasons for the discrepancy could be: 1) penetration of tephra particles through the lake sediment, or 2) wedging of older material into the younger deposits due to some mudflows or underwater landslides. The first reason is favored because neither visual inspection nor instrumental investigations reveal any disturbance or sharp changes in character of the deposits

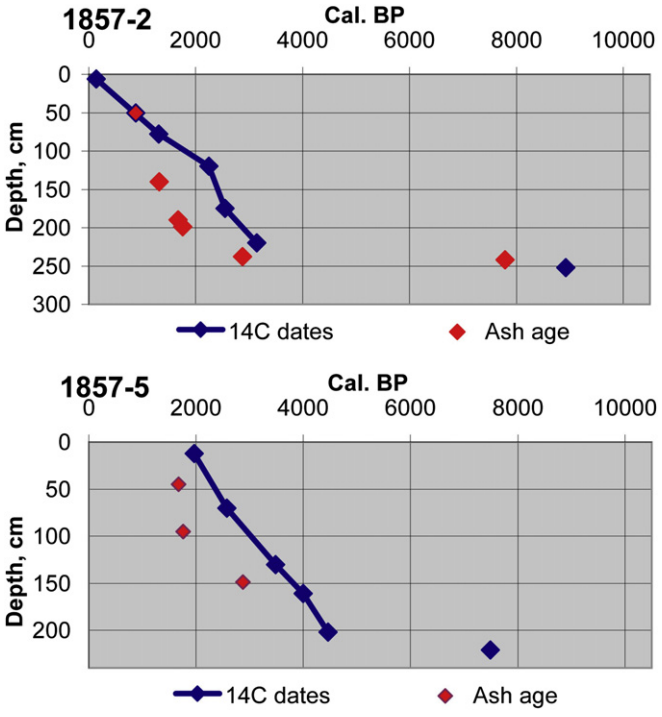

Fig. 10. Depth-age curves for cores 1857/2 and 1857/5.

within the inspected interval. Moreover, the results of radiocarbon dating did not reveal any reservoir effect (see Fig. 7). Random admixtures of older organic material in the younger lake deposits would have resulted in more inconsistent depth-age curves for both 1857/2 and 1857/5 lake cores. The soupy consistency of the lacustrine deposits could facilitate the tephra sinking through them during or just after deposition. Additionally, most of the tephras demonstrate a depth of submergence of the same order of magnitude, in range 60–100 cm, also supporting the idea of sinking. Similar submergence of distal tephras with greater age amplitude was reported by Beierle and Bond (2002) in the Copper and Doal lakes, Canada.

The presence of the older tephras at the base of core 1857/2 could be explained by a hiatus in its lower part, clearly shown by the tephra stratigraphy and the results of radiocarbon dating (Fig. 10). The origin of this hiatus is discussed in Section 4.6.

4.5. Landscape development

As a result of tephrochronological investigation of terrestrial sections, ten distal tephras of four volcanoes (Table 2) can be used as chronological marker tephra layers. These tephra layers as well as several radiocarbon dates allowed reconstruction of the main paleoenvironmental events in this area during the late Pleistocene – Holocene.

Several paleolandslides occurred around the lake (Fig. 11). Their size and position indicate strong impacts of these landslides on the lacustrine environment at the lake depression. Dating of these events is of special importance because it helps to exclude any landslide-related disturbances of paleoenvironments from paleoclimatic records.

The largest landslide occurred from the SE side of the TYL depression and filled the valley. Its deposit dammed the valley, forming TYL. In the proximal 7 km it has a typical chaotic hummocky relief with relative height of the hummocks up to 15 m. The distal part is represented with scattered isolated hills as high as 20 m. Some of the hollows are presently occupied by small lakes. The maximum travel distance of the landslide was about 10.5 km and maximum drop height was 0.65 km. Total area of the landslide deposits is about 22 km^2. Considering the average initial thickness of the deposit to be 15 m, the volume of the landslide is about 0.3 km^3, placing this as a large non-volcanic landslide (Legros, 2002; Ponomareva et al., 2006). The landslide was a result of a sliding of the thick sequence (up to 50 m) of Early Pleistocene subhorizontal lava flows which cover poorly consolidated pyroclastic deposits (Ogorodov, 1972). For the initial 4 km of the landslide route, it propagated NW, but made an almost 90° turn to the NE as it touched the opposite side of the valley. In spite of a relatively small drop height, the travel distance was rather long compared to other subaerial landslides (Legros, 2002).

Considering the absence of direct radiocarbon dating of this landslide, its age could be assumed based on several observations. The upper age limit of the event is defined by the age of soil-pyroclastic sequence at the surface of the landslide deposits (site 200,723, Fig. 3). Based on two radiocarbon dates (8320 ± 50 BP and 8360 ± 50 BP), the landslide could have occurred in the Late Pleistocene – very Early Holocene. The rather fresh appearance of the landslide relief excludes erosion by glaciers, which existed here during the LGM. Some additional estimation could be suggested after consideration of the characteristic features of the landslide. The rather long travel distance suggests that friction forces were significantly reduced during the landslide movement. The presence of a glacier at that time could be the reason for such reduction. This glacier, however, was not active, preventing transport to the terminal moraines. The appearance of the terminal part of landslide as scattered isolated hills suggests the intense sculpturing the landslide deposits by a proglacial lake, formed during glacial melting. In addition, the intense melting of the glacier during its retreat could remove the loose pyroclasts, described in the middle part of the surrounding valley walls (Ogorodov, 1972) and facilitate the avalanching of the brittle Early Pleistocene lava apron which constitutes the uppermost part of the valley slopes. These data place the landslide in the Late Pleistocene, soon after the start of LGM glacier retreat, probably ca. 15,000–18,000 ^{14}C BP. However, the exact age of this event requires additional study.

Another landslide affected the ESE lake shore. The landslide has a typical chaotic hummocky relief with relative height of the hummocks up to 5 m, and some small lakes in the interhummock depressions. The source area of this landslide abuts with the scarp of the Late Pleistocene landslide described above. The maximum drop height is 0.65 km, and the maximum subaerial travel distance is about 3 km. The TYL bathymetry revealed an underwater bulge (Figs. 1 and 11) at the east part of the lake bottom, believed to be a distal part of the landslide. Considering this, the total travel distance is 4 km, the area of the landslide deposits is about 5 km^2 and volume is about 0.05 km^3 (assuming an average thickness of the deposits of 10 m; Table 3).

The age of this event was obtained from several observation sites near the lake (Fig. 3) by tephrochronology and radiocarbon dating. At the surface of the landslide deposits (site 200,724, Fig. 12, left photo), tephra KL ca. 2850 ^{14}C BP lies directly on top of the landslide deposits. At site 200,721 (Fig. 12, right photo), on the flank, where its deposit is 20 cm thick strata of angular blocks up to 20 cm in size, the oldest tephra is SH_{2800}. These data suggest that the landslide took place about 2900 ^{14}C BP.

Table 2
Holocene marker ash layers identified in terrestrial sections around Two-Yurts lake.

Eruptive center	Code	Field code	Age, ^{14}C BP	Average glass composition	General crystal assemblage	Characteristic features	
Shiveluch	SH_2	21/2	965 ± 16	Rhyolite	Pl/GHb/Mt/OPx/CPx/BHb	Medium-K_2O content,	presence of Ol
	SH_3	–	1404 ± 27	Rhyolite	Pl/Hb/Px/Mt/Ol	prevalence of GHb over	
	SH_3^a	23/1	ca. 1750	Rhyolite	Pl/GHb/Mt/OPx/CPx/BHb	other heavy minerals	presence of Ol
	SH_{2800}	21/4	ca. 2800	Rhyolite	Pl/GHb/Mt/OPx/BHb/CPx/Ap		
	SH_{4700}	23/7	ca. 4700	Rhyolite	Pl/GHb/Mt/OPx/CPx/BHb/Ol		
	SH_{4800}	23/6	ca. 4800	Rhyolite	Pl/GHb/OPx/Mt/CPx/BHb/Ol		presence of Ol
	SH_{8300}	23/3	ca. 8300	Rhyolite	Pl/GHb/Mt/OPx/BHb/CPx		
Ksudach, caldera V	KS_1	21/3	1806 ± 16	Rhyolite	Pl/Px/Mt/Hb	Low K_2O content	
Klyuchev-skoy	KL	21/3	ca. 2850	Basalt?	Pl/Ol/OPx/CPx/Mt/BHb	Prevalence of Ol over other heavy minerals	
Khangar	KHG	23/5	6957 ± 30	Rhyolite	Pl/Hb/OPx/Bi/Mt	High K_2O content, presence of Bi, Hb	

Radiocarbon age for SH_2, SH_3, KS_1, and KHG ashes – according to Braitseva et al. (1997), for other ashes – see this paper, characteristics of SH_3 ash – according to Ponomareva et al. (2007). See text and Fig. 4 for mineral abbreviations.

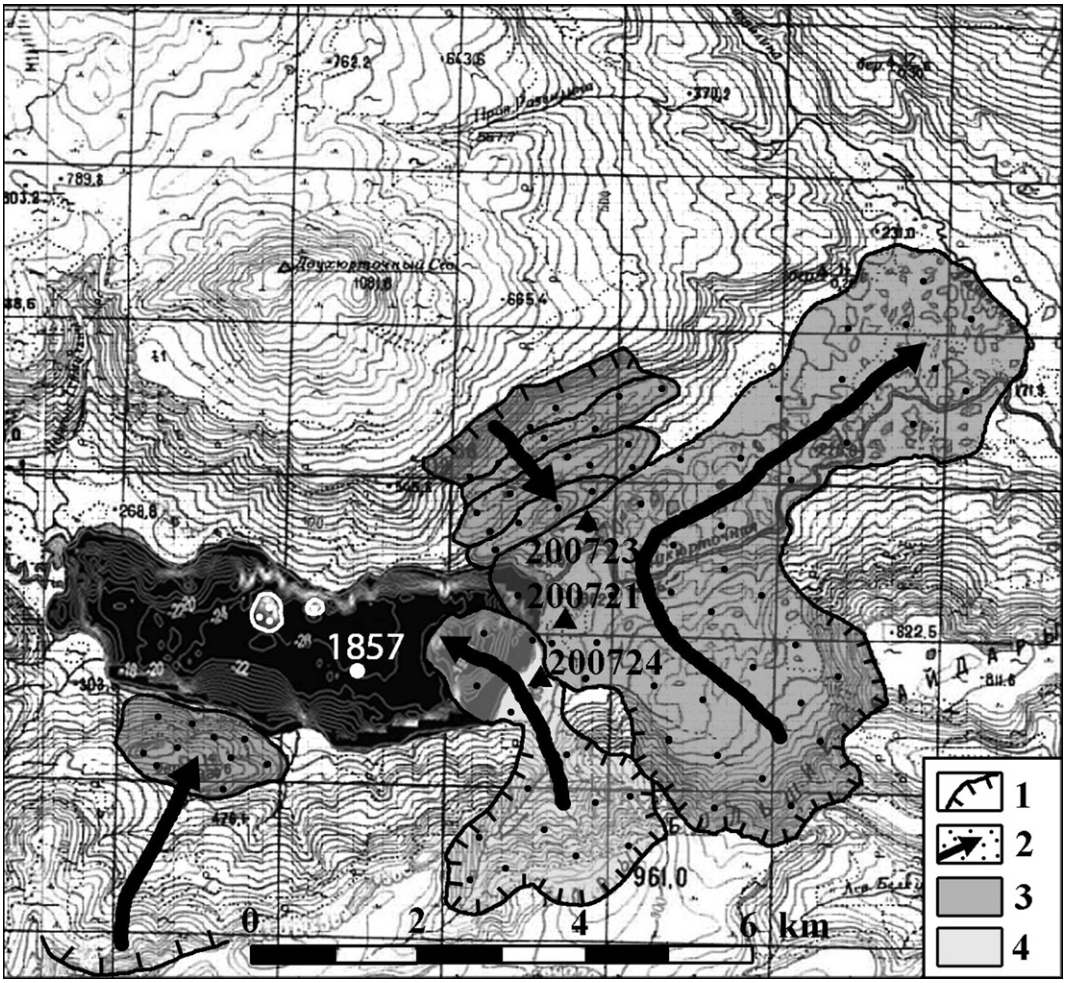

Fig. 11. Landslides in TYL area. 1 – source area of landslides, 2 – landslide deposits; age of landslides: 3 – Late Pleistocene, 4 – Holocene. Supposed landslide blocks at the lake bottom are outlined in white.

Several more landslides at Two-Yurts lake area were identified, but do not have reliable age data at present (Fig. 11). Two occurred at the SSW and NNE sides of the lake depression and represent intact blocks of lava plateau, which slid for distances 2–3 km. Their smooth relief probably indicates intense glacial erosion, i.e. they were formed before or during the LGM.

Inspection of the bathymetric map reveals several isolated blocks of isometric shape on the flat bottom of the lake along the north coast. The largest is 0.5 × 0.3 km and about 25 m thick. They probably represent small landslides from the steep northern flank of the lake depression. The isometric shape of these hummocks suggests an absence of glacial erosion and supports a Holocene age.

4.6. Late Holocene landslides and their impact: tsunami at Two-Yurts lake

The data suggest that a landslide ca. 2900 ^{14}C BP entered the lake and resulted in the formation of a tsunami in this non-volcanic lake. The deposits of this tsunami have been found at two sites. Along the eastern coast of the lake (site 200,721), they are represented as a discontinuous layer of structureless poorly sorted sand with dispersed rounded pebbles up to 1 cm in size, directly overlying the landslide deposits (Fig. 3). The tsunami spread all around the lake and propagated along the Two-Yurts River. Two kilometers downstream of the lake (site 200,723) tsunami deposits wedge into the typical terrestrial soil-pyroclastic sequence (Fig. 3). The tsunami deposits at this site consist of three layers (from bottom to top): 10 cm thick layer of structureless poorly sorted sand and dispersed pebbles up to 5 mm; 20 cm thick layer of poorly stratified moderately sorted sand; and 5–10 cm layer of poorly sorted sand and pebbles up to1 cm in size mixed with a sandy load with dispersed charcoal. This sequence is interpreted as a tsunami deposit (lowermost unit) covered by a lacustrine deposit (middle unit) of a short-lived lake which formed here after the flooding. The uppermost unit could represent slopewash material from the surrounding hills soon after the tsunami. The radiocarbon date of

Table 3
Parameters of some landslides, Two-Yurts lake area.

Age, ^{14}C BP	Drop height (H, km)	Maximum run-out (L, km)	H/L ratio	Area, km^2	Average thickness, m	Volume, km^3
15,000–18,000	0.65	10.5	0.07	22	15	0.33
2900	0.65	4	0.16	5	10	0.05

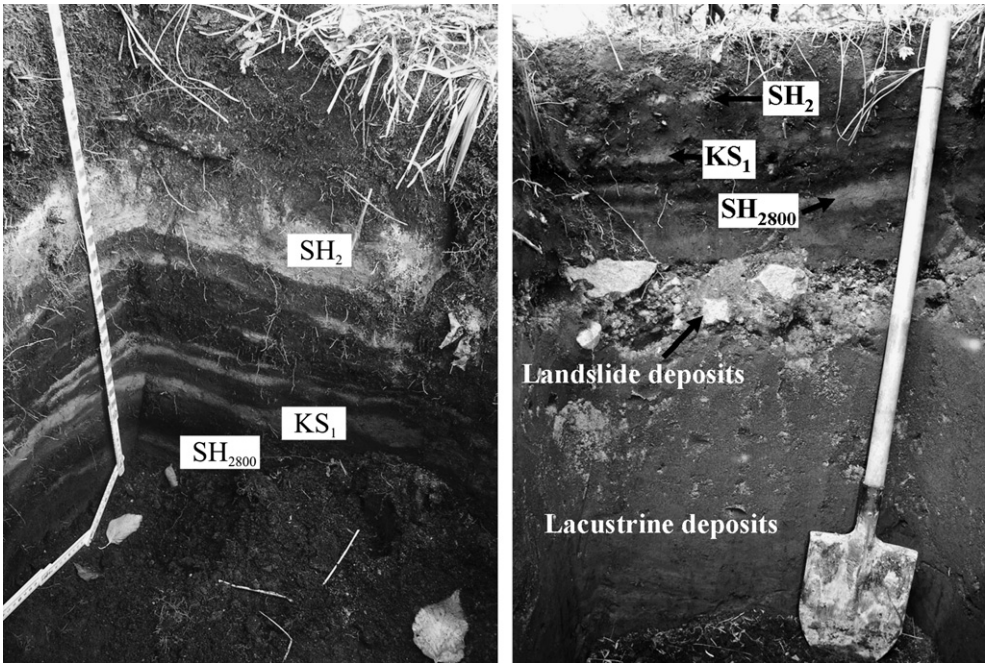

Fig. 12. Sections at Two-Yurts, situated at the surface of landslide deposits (left section) and at the most distal part of landslide propagation (right section). The shovel is ~1.2 m long.

2865 ± 35, yielded from the charcoals in this unit, corresponds well to the estimated age of the landslide. Further evidence of the tsunami was found in the sediment core obtained from Sigrid lake. Tephrochronological data indicates that the age of the lake is about 2900–3000 ^{14}C BP, as the oldest tephra layer, found near the basement of the core, is SH_{2800} tephra. This suggestion is supported by the diatom assemblage in the lower 3 cm of the core (Hoff et al., in press). The diatom composition is quite similar to the one of nearby TYL but strongly differs from the assemblage in the overlying section. The lowermost 3 cm of the core consists of reworked lacustrine sediments expelled by the tsunami from TYL. Two radiocarbon dates at the lowermost part of the core also indicate the presence of older (reworked) organic material which could be transported by the tsunami.

The estimation of the tsunami height at the lakes shores was done by analyzing the deposits at sites 200,721 and 200,724 and their recent relative elevations. Tsunami deposits were found at the surface of landslide deposits at site 200,721, but were absent in the contemporaneous deposits at site 200,724, which is ~5 m higher. This suggests that the height of tsunami did not exceed 5 m on the western shore. However the peak tsunami height in the narrow Two-Yurts River valley 2 km downstream of the lake (at site 200,723) exceeded 10 m, as this is the elevation of this site above the present-day level of the Two-Yurts River.

Deposits of two younger tsunami events are present. At site 200,721 (Fig. 3) there are two 5–10 cm thick layers of fine to coarse grained poorly sorted sand with admixture of well rounded pebbles up to 1 cm in size, interbedded between KS_1 and SH_{2800} tephras. These deposits were probably formed by redeposition of lake sediments by tsunami rather than other processes for several reasons. Storm-wave influence in the TYL is expected to operate by elevation and distance from the shoreline, generally not higher than 1 m and not greater than 10 m (indicated by the present-day position of the dense plant cover). Colluvium, mudflows, and landslide deposits are poorly sorted and have angular blocks, whereas eolian sands are typically very well-sorted. These tsunami could be formed by two landslides, which formed separated submerged blocks near the northern lake shore (see Section 4.5). The age of these landslides was determined by their stratigraphic position between the KS_1 and SH_{2800} tephras and one radiocarbon date of 2040 ± 35 BP obtained from the charcoals between these layers, defining the age of both events as 2000–2100 ^{14}C BP.

The tsunami waves also significantly disturbed the lake sediments. The wave propagation through the lake was accompanied by intense erosion of bottom sediments in some localities. In core 1857/2, SH_{2800} and KL tephras lie only 2 cm above KHG tephra, indicating either sharp reduction of the depositional rate for the time 3000–6900 ^{14}C BP or strong erosion about 3000 ^{14}C BP. This time corresponds very well to the suggested time of the landslide. Thus, the landslide was accompanied not only by a surface tsunami but also by strong underwater erosion.

A similar sharp decrease in depositional rate was observed also in the 1857/5 core for the interval between ca. 4000–6500 ^{14}C BP. In spite of the absence of a visually detected terrestrial landslide of this age, another landslide-tsunami event at ca. 4000 ^{14}C BP is suggested. This probably also reached the lake and caused another tsunami, and an underwater surge eroded the deposits. However the impacts of two other Holocene tsunami (2000–2100 ^{14}C BP) were not found in the lacustrine core. A smaller size of the sliding blocks probably resulted in weaker tsunami, if any, which did not erode lake deposits.

Thus, investigation revealed several landslides of different scales during the Late Pleistocene – Holocene. Some entered the lake to produce tsunami, which inundated the lake shores and in some cases eroded the lake sediments, creating breaks in depositional records. Understanding the nature of these breaks is important for paleoenvironmental research, to avoid attributing them to any climatic events resulting in cessation of sedimentation.

5. Conclusions

1. Seven main marker tephra layers originating from Shiveluch volcano, and three others from Ksudach, Klyuchevskoy and Khangar volcanoes, were identified and used for reconstruction of the Holocene history of landscape development.

2. The lacustrine sediments from Two-Yurts lake provided less favorable conditions for volcanic tephra preservation compared to terrestrial sections. In some case the tephras sank through the lake deposits, significantly impeding age determinations and use for paleoreconstructions. Thus, application of tephra layers as chronological markers for lacustrine deposits requires additional investigation to avoid distortion in depth-age models
3. Three landslides, including the largest one ca. 15,000–18,000 ^{14}C BP which resulted in the formation of TYL, occurred during the Late Pleistocene. Four Holocene landslides took place ca. 4000, 2900, 2100–2000 ^{14}C BP. All reached the lake and caused tsunami formation.
4. These tsunami waves not only affected terrestrial environments where they were as high as 10 m, but also significantly disturbed the lake sedimentation. They eroded the lake sediments and are expressed as sharp changes of sedimentation rates in depth-age models.

Acknowledgements

This research was possible thanks to cooperative German-Russian KALMAR project (BMBF 03G0640A,B) and grants from the Deutsche Forschungsgemeinschaft (DFG) and Russian Foundation for Basic Research (RFBR). We are very grateful to Conrad Copsch for the bathymetry map of TYL. We would like to express our gratitude to Dr. Yoshitaka Nagahtephrai who provided us with results of geochemical analyses of volcanic glasses. We also would like to thank Lilia Bazanova for help with tephra identification. The comments of anonymous reviewers were very useful and significantly improved the manuscript.

Appendix. Supplementary material

Supplementary material related to this article can be found online at doi:10.1016/j.quaint.2011.08.032.

References

Bazanova, L.I., Pevzner, M.M., 2001. Khangar: one more active volcano in Kamchatka. Transactions (Doklady) of the Russian Academy of Sciences. Earth Sciences 377A, 307–310.

Bazanova, L.I., Braitseva, O.A., Puzankov, M., Yu, Sulerzhitsky, L.D., 2003. Catastrophic plinian eruptions of the initial cone-building stage of the Young Cone of Avachinsky volcano (Kamchatka). Volcanology and Seismology 6, 20–40 (In Russian).

Bazanova, L.I., Braitseva, O.A., Melekestsev, I.V., Sulerzhitsky, L.D., 2004. Catastrophic eruptions of Avachinsky volcano (Kamchatka) in Holocene: chronology, dynamics, geological effect, environmental impact and long-term forecast. Volcanology and Seismology 6, 15–20 (In Russian).

Bazanova, L.I., Braitseva, O.A., Dirksen, O.V., Sulerzhitsky, L.D., Danhara, T., 2005. Tephrafalls from the largest Holocene eruptions along the Ust'-Bol'sheretsk - Petropavlovsk-Kamchatsky traverse: sources, chronology, recurrence. Volcanology and Seismology 6, 30–46 (In Russian).

Beierle, B., Bond, J., 2002. Density-induced settling of tephra through organic lake sediments. Journal of Paleolimnology 28, 433–440.

Bigg, G.R., Clark, C.D., Hughes, A.L.C., 2008. A last glacial ice sheet on the Pacific Russian coast and catastrophic change arising from coupled ice–volcanic interaction. Earth and Planetary Science Letters 265 (3–4), 559–570.

Bourgeois, J., Pinegina, T., Ponomareva, V., Zaretskaia, N., 2006. Holocene tsunami in the southwestern Bering Sea, Russian Far East, and their tectonic implications. Geological Society of America Bulletin 118, 449–463.

Braitseva O. A., Sulerzhitsky L. D., Egorova I.A., 1980. Tephrostratigraphy and radiocarbon dating. In: Masurenkov Yu.P. (Ed.), Volcanic center: structure, dynamics, products (Karymsky center), 90–100. (In Russian).

Braitseva, O.A., Kirianov, V.Yu., Sulerzhitsky, L.D., 1989. Marker intercalations of Holocene tephra in the Eastern volcanic zone of Kamchatka. Volcanology and Seismology 7, 785–814.

Braitseva, O., Melekestsev, I., Ponomareva, V., Yu, Kirianov, 1996. Caldera-forming eruption of Ksudach volcano ca 240 AD. Journal of Volcanology and Geothermal Research 70 (1–2), 49–65.

Braitseva, O.A., Ponomareva, V.V., Sulerzhitsky, L.D., Bailey, J., 1997. Holocene key-marker tephra layers in Kamchatka, Russia. Quaternary Research 47, 125–139.

Braitseva, O.A., Bazanova, L.I., Melekestsev, I.V., Sulerzhitsky, L.D., 1998. Largest Holocene eruptions of Avachinsky volcano, Kamchatka. Volcanology and Seismology 20, 1–27 (In Russian).

Danzeglocke U., Joris O., Weninger B., 2010. CalPal-2007. http://www.calpal-online.de/ (accessed 01.11.).

Dirksen, O.V., Melekestsev, I.V., 1999. Chronology, evolution and morphology of plateau basalts eruptive centers in Avacha river area, Kamchatka. Russia Volcanology and Seismology 21, 1–27.

Dirksen, O.V., Ponomareva, V.V., Sulerzhitsky, L.D., 2002. Eruption from Chtephraa Crater – a unique large silicic eruption at a monogenetic basaltic lava field. Volcanology and Seismology 5, 3–10 (In Russian).

Dirksen O., Danhara T., Takahara H., Ikeda Sh., Sasaki N., 2006. Tephrastratigraphy of Central Kamchatka peat sections – basement for detail paleoenvironmental research. Abstract of the 2nd Scientific Congress of East Asian Federation of Ecological Societies. Niigata, Japan. p. 459.

Hoff U., 2010. Freshwater diatoms as indicators for Holocene environmental- and climate changes on Kamchatka, Russia. PhD thesis, Potsdam University, Potsdam, Germany.

Hoff U., Dirksen O., Dirksen V., Herzschuh U., Hubberten H.-W., Meyer H., Ponomareva V., Bogaard van den C., Diekmann B., In press. Late Holocene diatom assemblage in a lake sediment record of central Kamchatka, Russia. Journal of Paleolimnology.

Krasheninnikov, S., Portnyagin, M., Ponomareva, V., Kuvikas, O., Mironov, N., 2009. Tephra records of volcanic activity in Klyuchevskoy Group of volcanoes during the Early Holocene. Terra Nostra 1, 44–45.

Kuehn S.C., Froese D.G., and Shane P.A.R., in press. The INTAV intercomparison of electron-beam microanalysis of glass by tephrochronology laboratories, results and recommendations. Quaternary International.

Kyle, P., Ponomareva, V., Rourke, R., 2011. Geochemical characterization of marker tephra layers from major Holocene eruptions, Kamchatka Peninsula, Russia. International Geology Review 53 (9), 1059–1097.

Legros, F., 2002. The mobility of long-runout landslides. Engineering Geology 63, 301–331.

Melekestsev, I.V., Ponomareva, V.V., Volynets, O.N., 1995. Kizimen volcano (Kamchatka) – future Mt. St.Helens? Journal of Volcanology and Geothermal Research 65, 205–226.

Melekestsev, I.V., Kurbatov, A.V., 1998. Frequency of large paleoearthquakes at the northwestern coast of the Bering Sea and in the Kamchatka Basin during late Pleistocene/Holocene time. Volcanology and Seismology 19, 257–267.

Nagahtephrai, Y., Yoshida, T., Nakai, S., Okudaira, T., 2003. Evaluation and correction of EDS results of the glass shards from some representation tephra by comparison with XRF analysis. Quaternary Research 42, 265–277.

Ogorodov, N., 1972. Volcanoes and Quaternary volcanism of Sredinny Range, Kamchatka. Nauka Publishers, Moscow, 190 pp. (In Russian).

Ozerov, A.Yu., Ariskin, A.A., Barmina, G.S., 1996. The problem of genetic relations between high-aluminous and high-magnesian basalts of the Klyuchevskoi volcano, Kamchatka, 350. Transactions (Doklady) of the Russian Academy of Sciences/Earth Science sections. 7; 1127–1130.

Pinegina, T., Bourgeois, J., Bazanova, L., Melekestsev, I., Braitseva, O., 2003. Millennial – scale record of Holocene tsunami on the Kronotskiy Bay coast, Kamchatka, Russia. Quaternary Research 59, 36–47.

Ponomareva, V.V., Pevzner, M.M., Melekestsev, I.V., 1997. Large debris avalanches and associated eruptions in the Holocene eruptive history of Shiveluch Volcano, Kamchatka, Russia. Bulletin of Volcanology 59 (7), 490–505.

Ponomareva, V., Melekestsev, I., Dirksen, O., 2006. Sector collapses and large landslides on late Pleistocene–Holocene volcanoes in Kamchatka, Russia. Journal of Volcanology and Geothermal Research 158 (1–2), 117–138.

Ponomareva, V.V., Kyle, P.R., Pevzner, M.M., Sulerzhitsky, L.D., Hartman, M., 2007. Holocene eruptive history of Shiveluch volcano. Kamchatka Peninsula. In: Eichelberger, J., Gordeev, E., Kasahara, M., Izbekov, P., Lees, J. (Eds.), Volcanism and Subduction: The Kamchatka Region. American Geophysical Union Geophysical Monograph Series, vol. 172, pp. 263–282.

Portnyagin, M., Ponomareva, V., Bindeman, I., Hauff, F., Krtephraeninnikov, S., Kuvikas, O., Mironov, N., Plechova, A., van den Bogaard, C., 2009. Millennial variations of major and trace element and isotope compositions of Klyuchevskoy magmas, Kamchatka. Terra Nostra 1, 64–65.

Savoskul, O., Zech, W., 1997. Holocene glacier advances in the Topolovaya valley, Bystrinskiy Range, Kamchatka, Russia, dated by tephrochronology and lichenometry. Arctic and Alpine Research 29, 143–155.

Volynets, O.N., Ponomareva, V.V., Braitseva, O.A., Melekestsev, I.V., Chen Ch., H., 1999. Holocene eruptive history of Ksudach volcanic massif, South Kamchatka: evolution of a large magmatic chamber. Journal of Volcanology and Geothermal Research 91 (1), 23–42.

Wetzler, N., Marco, S., Heifetz, E., 2010. Quantitative analysis of seismogenic shear-induced turbulence in lake sediments. Geology 38 (4), 303–306.